# Structure of $^{72,74}$Ge nuclei probed with a combined analysis of heavy-ion fusion reactions and Coulomb excitation

Muhammad Zamrun F.
*Jurusan Fisika FMIPA, Universitas Haluoleo, Kendari, Sulawesi Tenggara 93232, Indonesia*

Zakarya Mohamed Mohamed Mahmoud
*Department of Physics, Assuit University, Assuit, Egypt*

N. Takigawa[*] and K. Hagino
*Department of Physics, Tohoku University, Sendai 980-8578, Japan*

(Received 26 February 2010; published 20 April 2010)

We study the fusion reactions of the $^{72}$Ge + $^{72}$Ge and $^{74}$Ge + $^{74}$Ge systems in terms of the full order coupled-channels formalism. We obtain the fusion excitation function as well as the fusion barrier distribution of these reactions using the coupling matrix suggested from the recent Coulomb excitation experiments. We compare those results with the results obtained by the coupling matrix based on the pure vibrational and rotational models. The barrier distribution for the $^{74}$Ge + $^{74}$Ge reaction obtained with the experimental coupling matrix is in good agreement with that obtained with the vibrational model, in contrast to the rotational model. On the other hand, the calculations for $^{72}$Ge + $^{72}$Ge system show that the fusion barrier distribution obtained with the experimental coupling matrix significantly differs from those obtained with vibrational and rotational models. Our study indicates that the shape of $^{74}$Ge is closer to spherical than to deformed, while $^{72}$Ge has a shape admixture in its ground state, which can be described by neither the vibrational nor the rotational models, as suggested by the Coulomb excitation experiments. This finding will resolve the debates concerning the structure of these nuclei.

DOI: 10.1103/PhysRevC.81.044609 PACS number(s): 24.10.Eq, 25.60.Pj, 27.50.+e

## I. INTRODUCTION

It is now well established that the heavy-ion fusion reaction at energies near and below the Coulomb barrier is very sensitive to the structure of the colliding nuclei. In particular, the collective excitations (rotations and surface vibrations), neck formation, and/or nucleon transfer strongly influence the fusion cross section for intermediate mass systems [1–4]. The coupled-channels calculations [1,3,4] for the high-precision experimental data [2,5] of fusion reactions show that the structure of the colliding nuclei can be probed through the analysis of the so-called fusion barrier distribution which is defined as the second derivative of the product $E\sigma_{\rm fus}(E)$, $\sigma_{\rm fus}$ being the fusion cross section, with respect to the center-of-mass energy $E$, that is, $D^{\rm fus} = d^2(E\sigma_{\rm fus})/dE^2$ [6]. In addition to the conventional Coulomb excitation method, this method has been shown to provide an alternative useful means for determining the structure of nuclei.

In this paper, we study the $^{72}$Ge + $^{72}$Ge and $^{74}$Ge + $^{74}$Ge fusion reactions with a coupled-channels approach in order to probe the structure of $^{72,74}$Ge nuclei. This is motivated by the existence of debates concerning the structure of Ge isotopes. For example, the low-lying energy spectrum of the $^{74}$Ge nucleus [7] shows that its first excited state is a $2^+$ state with the excitation energy 0.595 MeV and there exist excited $0_2^+$, $2_2^+$, and $4_1^+$ states at energies nearly twice as high as that of the first $2^+$ state suggesting two phonon members. There also exists a low-lying $3^-$ state at energy 2.54 MeV. These facts indicate that $^{74}$Ge is a spherical nucleus, which is soft against deformation. A theoretical study of Ge isotopes by Dobaczewski *et al.* [8] using the Skyrme Hartree-Fock method also shows that the $^{74}$Ge has a spherical shape. The same conclusion is obtained also by the relativistic mean field calculations of Sharma *et al.* [9].

On the other hand, a series of experiments of Coulomb excitation [10–13] give an alternative point of view. They suggest that two different shapes coexist in the low energy region in each Ge isotope and that the shape of the ground state changes from a spherical shape to a deformed shape as the neutron number increases. The $^{74}$Ge is a transitional nucleus where the experimental ratio of $B(E2, 4_1^+ \to 2_1^+)/B(E2, 2_1^+ \to 0_1^+)$, $B(E2, 2_2^+ \to 2_1^+)/B(E2, 2_1^+ \to 0_1^+)$, and $B(E2, 0_2^+ \to 2_1^+)/B(E2, 2_1^+ \to 0_1^+)$ are 1.3, 0.84, and 0.30, respectively, in disagreement with the vibrational model which predicts all of these ratios to be 2 [12]. The $^{72}$Ge is suggested to have a large shape admixture [13].

The idea of the shape transition has been tested through the analysis of the fusion excitation functions of $^{16}$O,$^{27}$Al + $^{70,72,73,74,76}$Ge reactions [14,15]. Based on the analysis using the simplified coupled-channels code CCFUS, the authors claim that the shape changes from a spherical (or oblate) shape in $^{70,72,73}$Ge to a prolate shape in $^{74,76}$Ge. In Ref. [16], Esbensen has performed a more detailed coupled-channels calculations for the fusion excitation functions for the $^{16}$O,$^{27}$Al + $^{70,72,74,76}$Ge reactions and obtained the results that the phonon coupling model yields a smaller $\chi^2$ value than the rotational coupling model for $^{74}$Ge while the rotational coupling is preferred for $^{72}$Ge. He also concluded

[*]Center of General Education, Tohoku Institute of Technology, 982-8577 Sendai, Japan

 

that the quadratic coupling is required to obtain a good agreement between the coupled-channels calculations and the experimental data. Recently, Esbensen also analyzed the fusion excitation function of $^{74}$Ge + $^{74}$Ge reaction, and again claims that the vibrational coupling model gives a smaller $\chi^2$ value and that the inclusion of multiphonon excitations improves the agreement between theory and experiments [17,18].

Another interesting related analysis has been reported by Aguiar *et al.* [19]. They performed a systematic analysis of the so-called asymptotic energy shift, which is used as a measure of the enhancement of the fusion cross section at energies below the Coulomb barrier, for many systems along the periodic table. They found that the asymptotic energy shift for the $^{74}$Ge + $^{74}$Ge reaction significantly deviates from the systematics. It resembles the case for $^{40}$Ar + $^{154}$Sm system, whose large deviation from the systematics is probably caused by the coupling to the ground state rotational band of the target nucleus $^{154}$Sm. The study of Aguiar *et al.* suggests either the structural resemblance of $^{74}$Ge to $^{154}$Sm, i.e., that $^{74}$Ge is deformed, or the important role played by the dynamical deformation as argued in Ref. [20].

In this paper, we carry out detailed full order coupled-channels calculations for the $^{74}$Ge + $^{74}$Ge reactions and discuss the shape of $^{74}$Ge nucleus through the analysis of the fusion barrier distribution. The possibility of probing the shape admixture in $^{72}$Ge will also be discussed by analyzing the fusion barrier distribution for the $^{72}$Ge + $^{72}$Ge reactions. The preliminary results of this study have been published as a conference report in Ref. [21]. In this paper, we extend the calculations in Ref. [21] by enlarging the model space with respect to the partial wave sum and also by including the effects of higher levels such as the three-phonon quadrupole excitations of $^{74}$Ge.

The paper is organized as follows. We explain the parametrization for the interaction between two nuclei in Sec. II. The results of coupled-channels calculations are given in Sec. III. We summarize the paper in Sec. IV.

## II. PARAMETRIZATION OF THE INTERACTION

In performing the coupled-channels calculations, we introduce the no-Coriolis (the isocentrifugal) approximation to reduce the dimension of coupled-channels calculations [1,22–24]. Following Ref. [24], the coupling part of the total nucleus-nucleus interaction is given by

$$V_{\rm coup}(r, \hat{O}_{\lambda_P}, \hat{O}_{\lambda_T}) = V_C(r, \hat{O}_{\lambda_P}, \hat{O}_{\lambda_T}) + V_N(r, \hat{O}_{\lambda_P}, \hat{O}_{\lambda_T}), \quad (1)$$

$$V_C(r, \hat{O}_{\lambda_P}, \hat{O}_{\lambda_T}) = \left[\frac{3R_P^{\lambda_P}\hat{O}_{\lambda_P}}{(2\lambda_P+1)r^{\lambda_P}} + \frac{3R_T^{\lambda_T}\hat{O}_{\lambda_T}}{(2\lambda_T+1)r^{\lambda_T}}\right] \times \frac{Z_P Z_T e^2}{r}, \quad (2)$$

$$V_N(r, \hat{O}_{\lambda_P}, \hat{O}_{\lambda_T}) = \frac{-V_0}{\{1+\exp[\frac{r-R_0-(R_P\hat{O}_{\lambda_P}+R_T\hat{O}_{\lambda_T})}{a}]\}} - \frac{-V_0}{\{1+\exp[\frac{r-R_0}{a}]\}}. \quad (3)$$

TABLE I. The depth parameters of the nuclear potential for the $^{74}$Ge + $^{74}$Ge and $^{72}$Ge + $^{72}$Ge systems. The radius and the diffuseness parameters are taken to be $r_0 = 1.14$ fm and $a = 0.63$ fm, respectively, for both systems. The resultant Coulomb barrier height $V_B$ in MeV is also listed.

| System | $V_0$ (MeV) | $V_B$ (MeV) |
|---|---|---|
| $^{74}$Ge + $^{74}$Ge | 147.5 | 121.70 |
| $^{72}$Ge + $^{72}$Ge | 145.5 | 122.80 |

Here, $r$ is the distance between the center of mass of the projectile and target nuclei. $\hat{O}_{\lambda_P}$ and $\hat{O}_{\lambda_T}$ are the excitation operators in the projectile and target nuclei with multipolarity $\lambda_{(P,T)}$, respectively. $R_P$ and $R_T$ denote the coupling radii of the projectile and target nuclei, respectively. The $R_0$ is taken to be $r_0(A_P^{1/3} + A_T^{1/3})$. The second term on the right-hand side of Eq. (3) is the bare nuclear potential. It is subtracted in order to avoid double counting.

We apply this formalism to performing the coupled-channels calculations for the $^{74}$Ge + $^{74}$Ge and $^{72}$Ge + $^{72}$Ge fusion reactions. The numerical calculations are performed based on the CCFULL computer code [24]. We consider only the quadrupole coupling $\lambda = 2$ and determine the matrix elements of the operator $\hat{O}_{\lambda_{(P,T)}}$ in Eqs. (2) and (3) either from the experimental data of Coulomb excitation [12,13] or based on the collective vibrational or rotational coupling models [24]. We use the standard value for the diffuseness parameter, $a = 0.63$ fm, [25–28] and take the radius parameter to be $r_0 = 1.14$ fm. We adjust the depth parameter $V_0$ to reproduce the Coulomb barrier height given by Akyüs-Winther potential [25,26]. The resultant value of the depth parameter and the Coulomb barrier height are listed in Table I. The coupling radii of the projectile and target nuclei are taken to be $R_P = 1.2A_P^{1/3}$ and $R_T = 1.2A_T^{1/3}$, respectively.

## III. COUPLED-CHANNELS CALCULATIONS

### A. Probe of the structure of $^{74}$Ge nucleus

We now present the results of our coupled-channels calculations. We start from the discussion of the fusion between two $^{74}$Ge nuclei. Our interest is to examine whether the analysis of the fusion cross section can reveal the structure of $^{74}$Ge. The matrix elements of the coupling operator $\hat{O}_{\lambda_{(P,T)}}$ in Eqs. (2) and (3) obtained from the Coulomb excitation experiments [12] read

$$O_{ij} = \frac{\beta_2}{\sqrt{4\pi}}\begin{bmatrix} 0.0 & 1 & 0.102 & 0.0 & 0.0 \\ 1 & 0.243 & -0.489 & 0.827 & 0.253 \\ 0.102 & -0.489 & -0.316 & 0.046 & 0.0 \\ 0.0 & 0.827 & 0.046 & ? & 0.0 \\ 0.0 & 0.253 & 0.0 & 0.0 & 0.0 \end{bmatrix} \quad (4)$$

with the quadrupole deformation parameter $\beta_2 = 0.284$ for the low lying states arranged in the order of $0_1^+$, $2_1^+$, $2_2^+$, $4_1^+$, and $0_2^+$. In Eq. (4) and in the following the question marks and $\otimes$ in the experimental coupling matrices mean the absence of data. In this paper, we set them to zero.

We rewrite the matrix in Eq. (4) in a form of

$$O_{ij} = \frac{\beta_2}{\sqrt{4\pi}} \begin{bmatrix} 0 & 1 & 0 & 0 & 0 \\ 1 & 0 & -\sqrt{\frac{4}{7}} \times \underline{0.65} & \sqrt{\frac{36}{35}} \times \underline{0.84} & \sqrt{\frac{2}{5}} \times \underline{0.40} \\ 0 & -\sqrt{\frac{4}{7}} \times \underline{0.65} & 0 & 0 & 0 \\ 0 & \sqrt{\frac{36}{35}} \times \underline{0.84} & 0 & 0 & 0 \\ 0 & \sqrt{\frac{2}{5}} \times \underline{0.40} & 0 & 0 & 0 \end{bmatrix} \tag{5}$$

in order to compare with that for the harmonic vibrational model truncated by the two phonon states. The underlined numbers are the multiplication factors which are required to reproduce the experimental matrix elements given by Eq. (4). Alternatively, it can be rewritten as

$$O_{ij} = \frac{\beta_2}{\sqrt{4\pi}} \begin{bmatrix} 0.0 & 1.0 & 0.0 \\ 1.0 & \frac{2\sqrt{5}}{7} \times \underline{0.380} & \frac{6}{7} \times \underline{0.965} \\ 0.0 & \frac{6}{7} \times \underline{0.965} & \otimes \end{bmatrix} \tag{6}$$

in order to compare with the rotational coupling model including the first three states $0_1^+$, $2_1^+$, and $4_1^+$. Similarly to Eq. (5), the underlined numbers represent the modification factors from the pure rotational coupling model. Equations (5) and (6) clearly show the transitional property of $^{74}$Ge nucleus. Particularly, the reorientation matrix element in Eq. (6) is only about 38% of the pure rotational model.

Let us first discuss the results of two-level calculations, where the coupling to the intrinsic excitation of the projectile and target nuclei is truncated by the first excited $2^+$ state. Figure 1(a) shows the excitation function of the fusion cross section, while Figure 1(b) the fusion barrier distribution. The solid line is for the first $(2 \times 2)$ experimental coupling matrix given in Eq. (4), in which TS stands for "transitional structure." The dotted and dashed lines are for the pure vibrational and rotational models, respectively. The dot-dashed line is the result when both the target and projectile are assumed to be inert.

The excitation function of the fusion cross section obtained with the experimental coupling matrix resembles that for the rotational model at energies below $E_{\mathrm{c.m.}} = 115$ MeV, while it resembles that for the pure vibrational model for energies between $E_{\mathrm{c.m.}} = 115$ MeV and $E_{\mathrm{c.m.}} = 130$ MeV. At energies above $E_{\mathrm{c.m.}} = 130$ MeV, all the three calculations give similar results. Therefore, within the two level calculations, the fusion excitation function can hardly judge which of the vibrational or the rotational models better describes the structure of $^{74}$Ge. The situation does not change for the fusion barrier distribution. The fusion barrier distribution for the experimental coupling matrix has similar structure to that for both the vibrational and rotational models. It is shifted by nearly the same amount of energy from that for both the vibrational and the rotational models.

We next compare in Fig. 2 the results of coupled-channels calculations using the full five-dimensional experimental coupling matrix of Eq. (4) (solid line) with those obtained in the pure vibrational model truncated by the double phonon states (dotted line), and with those for the ground state rotational coupling model truncated at the $4^+$ member (dashed line). Figures 2(a) and 2(b) show the excitation function of the fusion cross section and the fusion barrier distribution, respectively. The interrelation among the three calculations remain qualitatively similar to that in the two channel calculations concerning

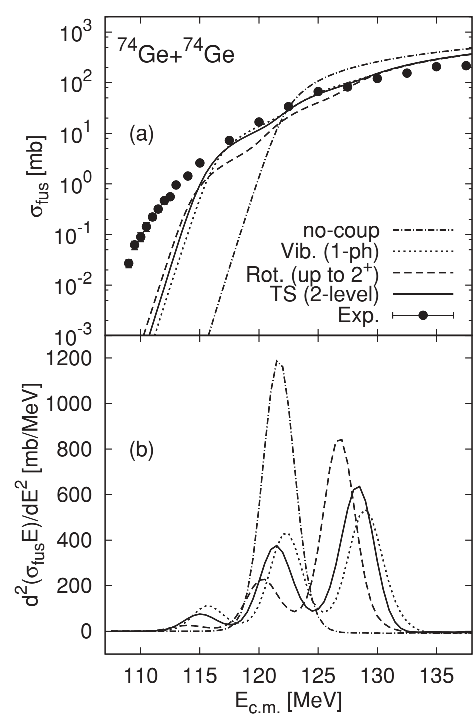


FIG. 1. Comparison of (a) the excitation function of the fusion cross section and (b) the fusion barrier distribution for the $^{74}$Ge + $^{74}$Ge reactions obtained with three different two-level calculations. The solid line is obtained with the experimental coupling matrix ("TS" stands for "transitional structure"), while the dotted and the dashed lines are with the pure vibrational and rotational models, respectively. The dot-dashed line is for the one dimensional calculation. Experimental data are taken from Ref. [29].

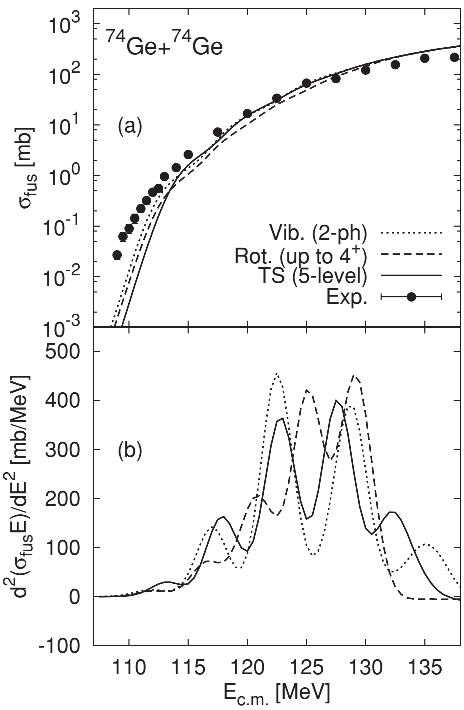


FIG. 2. Comparison of (a) the excitation function of the fusion cross section and (b) the fusion barrier distribution for the $^{74}Ge + ^{74}Ge$ reactions calculated in different models. The solid line is obtained by using the full five-dimensional experimental coupling matrix given in Eq. (4). The dotted line is obtained for the pure vibrational model including up to the double phonon states, while the dashed line for the rotational model including the coupling up to $4^+$ member of the ground state rotational band. Experimental data are taken from Ref. [29].

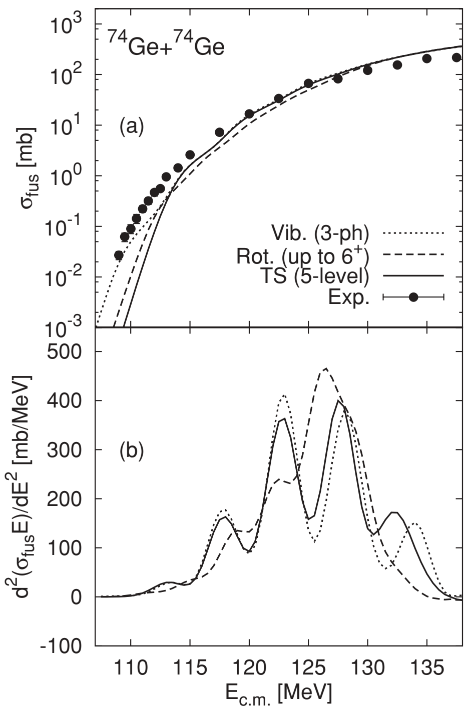


FIG. 3. The same as Fig. 2 but when the coupling up to the triple quadrupole phonon states in the vibrational model and the coupling up to the $6^+$ member of the ground state rotational band in the rotational coupling model are taken into account. Experimental data are taken from Ref. [29].

the excitation function of the fusion cross section, though they appear to have become closer to each other. On the other hand, the fusion barrier distribution clearly shows that the vibrational model agrees much better than the rotational model with the experiments, i.e., the fusion barrier distribution obtained in the vibrational model agrees much better than that in the rotational model with the fusion barrier distribution obtained by using the experimental coupling matrix.

It has been shown in Refs. [17,18] that the inclusion of the coupling to the triple quadrupole phonon states in the coupled-channels calculations in the vibrational model significantly improves the agreement with the experimental data of the fusion cross section of two $^{74}$Ge nuclei at energies near and below the Coulomb barrier. Therefore, here we examine the effects of this coupling on the fusion cross section and on the fusion barrier distribution. The results are given by the dotted line in Figs. 3(a) and 3(b) for the excitation function of the fusion cross section and the fusion barrier distribution, respectively. For comparison, we also show the results of the rotational coupling model when the coupling up to $6^+$ state is taken into account by the dashed line. The solid line is the same as in Fig. 2. We observe that the vibrational coupling model better agrees than the rotational model with the experimental coupling model concerning the excitation function of the fusion cross section at energies near and below the Coulomb barrier, which locates at $V_B = 121.7$ MeV, except for the energy region far below the Coulomb barrier. This reflects clearly also on the fusion barrier distribution. The good agreement of the fusion barrier distribution in the vibrational model with that for the experimental coupling demonstrated in Fig. 2(b) has been even more improved by the inclusion of the triple quadrupole phonon coupling. We have confirmed that, on the other hand, the poor agreement of the fusion barrier distribution in the rotational coupling model with that obtained by the experimental coupling matrix is not improved even if the coupling to the $8^+$ state is included. To be consistent with the conclusion in [17,18], these results favor a spherical shape more than a deformed shape for the ground state of $^{74}$Ge, although the actual coupling scheme is quite complicated and transitional.

It is well known that low-lying octupole excitations play an important role in sub-barrier fusion for many systems [5,30–32]. The octupole excitation, $3^-$ state, of $^{74}$Ge has the excitation energy of 2.54 MeV with the octupole deformation, $\beta_3 = 0.145$ [33]. Therefore, we also perform the coupled-channels calculations by including simultaneously the octupole coupling and the quadrupole excitations given by Eq. (4), although Eq. (4) was determined without considering the octupole excitation. The results are shown by dashed line in Figs. 4(a) and 4(b) for the fusion cross section and the fusion barrier distribution, respectively. The agreement with experimental fusion cross section is improved as compared with the results given by the experimental coupling matrix of Eq. (4) alone (solid line). A further improvement might

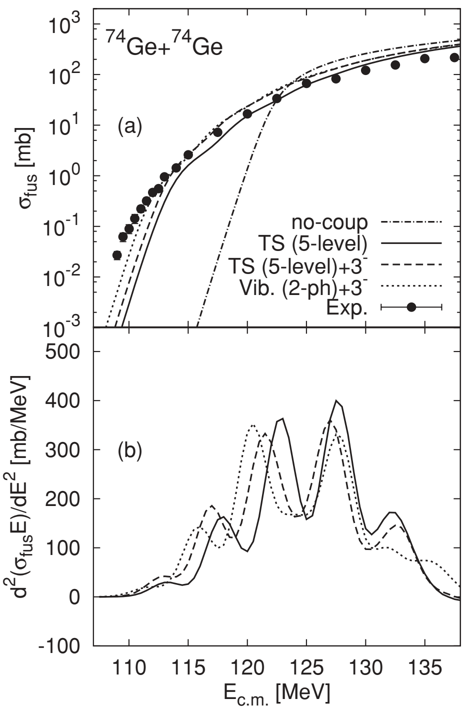


FIG. 4. Effect of octupole excitation on (a) the fusion excitation function and (b) the fusion barrier distribution for the reaction between two $^{74}$Ge nuclei. The solid line is the same as Fig. 2. The result of calculations which include the octupole vibration together with the experimental coupling of Eq. (4) is denoted by the dashed line and that with the pure double quadrupole couplings by the dashed line. The dotted-dashed line is the same as in Fig. 1. Experimental data are taken from Ref. [29].

be achieved if the effect of dynamical deformation argued in Ref. [20] is taken into account. For comparison, we also show the results of pure vibration model when the coupling to octupole excitation is taken into account in addition to the double quadrupole phonon couplings (the dotted line). The resultant fusion barrier distributions are qualitatively similar to those shown in Figs. 2 and 3. Our conclusions in Figs. 2 and 3 thus remain unchanged even with the octupole excitation. We have checked that the situation remains the same even if the coupling to the triple quadrupole phonon states together with the octupole phonon excitation is taken into account. These results strongly suggest that $^{74}$Ge has a spherical shape in its ground state.

### B. Probe of shape admixture in the ground state of $^{72}$Ge nucleus

We now discuss the effects of the shape admixture in $^{72}$Ge which has been discussed in Ref. [13]. Reference [13] argues that the ground state $0_1^+$, the first excited $0^+$ state, $0_2^+$, at 0.70 MeV, the first $2^+$ state, $2_1^+$, at 0.83 MeV and the third $2^+$ state, $2_3^+$, at 2.40 MeV are admixtures of two different shapes,

$$|0_1^+\rangle = \alpha|0_n^+\rangle + \sqrt{1-\alpha^2}|0_i^+\rangle, \tag{7}$$

$$|0_2^+\rangle = \sqrt{1-\alpha^2}|0_n^+\rangle - \alpha|0_i^+\rangle, \tag{8}$$

$$|2_1^+\rangle = \beta|2_n^+\rangle + \sqrt{1-\beta^2}|2_i^+\rangle, \tag{9}$$

$$|2_3^+\rangle = \sqrt{1-\beta^2}|2_n^+\rangle - \beta|2_i^+\rangle, \tag{10}$$

where the indices $n$ and $i$ stand for normal and intruder, respectively. According to Ref. [13], $\alpha = 0.784$, $\beta = 0.996$, and the normal and the intruder states are deformed and almost spherical, respectively. The corresponding experimental quadrupole coupling matrix is given to be

$$O_{ij} = \frac{\beta_2}{\sqrt{4\pi}}\begin{bmatrix} 0.0 & 0.0 & 1 & 0.025 \\ 0.0 & 0.0 & 0.781 & 0.140 \\ 1 & 0.781 & ? & 0.0 \\ 0.025 & 0.140 & 0.0 & ? \end{bmatrix} \tag{11}$$

with $\beta_2 = 0.242$ when the energy levels are arranged in the order of $0_1^+$, $0_2^+$, $2_1^+$, and $2_3^+$ states.

We have calculated the fusion cross section and the fusion barrier distribution for the $^{72}$Ge + $^{72}$Ge reactions by assuming the coupling matrix given by Eq. (11). The results are shown by the solid lines in Fig. 5 ("SA" stands for "shape admixture"). The dotted lines are obtained with the pure vibrational model truncated by the one phonon state. The dashed lines denote the results of the pure rotational model truncated by the $2^+$ member of the ground state rotational band. The dot-dashed lines represent the results of one dimensional calculation.

Neither the vibrational model nor the rotational model can well reproduce the fusion excitation function predicted by the

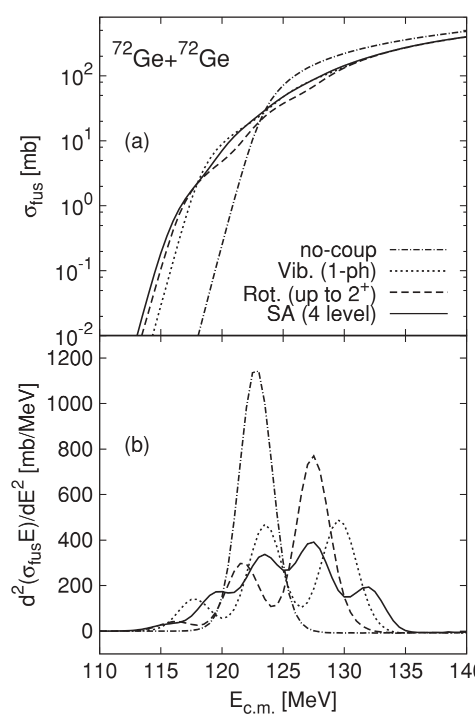


FIG. 5. Comparison of (a) the fusion cross section and (b) the fusion barrier distribution obtained with different models for $^{72}$Ge + $^{72}$Ge reactions. The dotted and dashed lines are obtained by the two-channel calculations with the vibrational and rotational models, respectively. The solid line is obtained by assuming the coupling matrix given in Eq. (11) ("SA" stands for "shape admixture"). The dot-dashed line is the result of one dimensional calculation.

experimental coupling Eq. (11) over the whole energy region. The rotational model reproduces the fusion excitation function predicted by the experimental coupling (solid line) at energies below $E_{\rm c.m.} = 118$ MeV better then the vibrational coupling. For energies between $E_{\rm c.m.} = 118$ MeV and $E_{\rm c.m.} = 130$ MeV, on the other hand, the vibrational model works better, i.e., the vibrational model reproduces the fusion excitation function predicted by the experimental coupling (solid line) better than the rotational model. The fusion excitation functions of all the three calculations merge at high energies, i.e., for energies above $E_{\rm c.m.} = 130$ MeV, as expected. The difference among the three calculations can be seen clearly also in the fusion barrier distributions.

Although Fig. 5(b) seems to suggest that the analysis of fusion reactions is promising to probe the shape admixture in $^{72}$Ge, one has to examine whether the significant difference of the fusion barrier distribution among different models persists even after one takes higher levels into account. In order to learn the situation, we extended calculations by including the coupling up to double quadrupole phonon states in the vibrational model. The results are given by the dotted lines in Fig. 6. The rotational coupling model has also been extended to include the coupling up to the $4^+$ state, and the results are given by the dashed lines in Fig. 6. The solid lines are the same as in Fig. 5.

The fusion excitation function and the fusion barrier distribution calculated in the vibrational and the rotational model, especially those by the latter, now agree somewhat better with those predicted by the experimental coupling matrix Eq. (11). However, the deviation is still fairly significant.

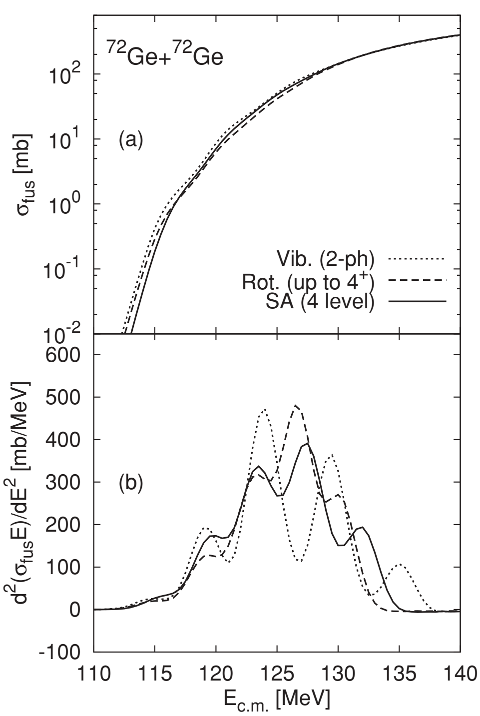


FIG. 6. The same as Fig. 5, but when the vibrational model is extended to include up to two phonon states, and the rotational coupling model up to the $4^+$ member of the ground states rotational band. The solid line is the same as that in Fig. 5.

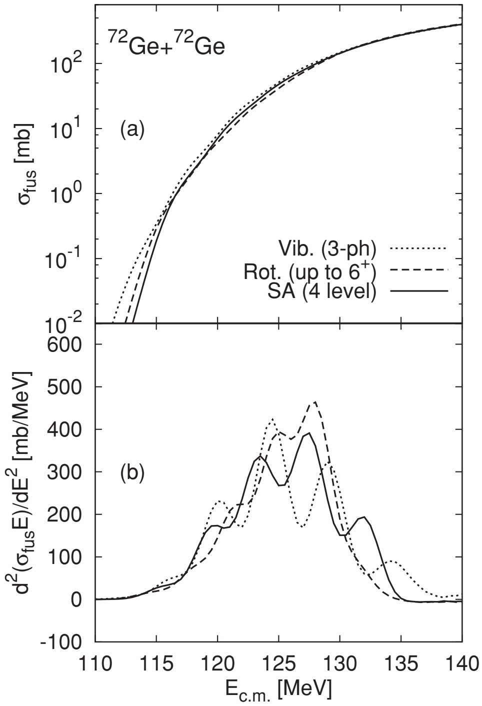


FIG. 7. The same as Fig. 6, but when the coupling up to the triple quadrupole phonon states for the vibrational model and the coupling up to the $6^+$ member of the ground state rotational band for the rotational coupling model are taken into account.

We further study whether the situation is still the same even if we take into account the coupling to higher levels. We show in Fig. 7 the results when the coupling up to the $6^+$ member of the ground state rotational band in the rotational coupling model and the coupling up to the three phonon states in the vibrational coupling model are taken into account by the dashed and dotted lines, respectively. The solid lines are the same as those in Fig. 6. Figure 7(b) shows that the agreement between the experimental fusion barrier distribution, i.e., the fusion barrier distribution predicted by Eq. (11), and that obtained by pure either vibrational or rotational models is not improved, or rather gets worse when the higher excited states are included. We have confirmed that the situation does not change even when the coupling up to the $8^+$ state is taken into account in the rotational coupling model. These studies suggest that it is hard to assign a particular shape, neither spherical nor deformed, to $^{72}$Ge, as has been claimed to be a shape-admixed state from the data of Coulomb excitation. In this connection, it will be interesting to experimentally determine the fusion barrier distribution, and to confirm whether it resembles in reality the solid line in Figs. 5 through 7. This will shed a further light on the shape admixture of $^{72}$Ge in addition to the experiments of the Coulomb excitation.

## IV. CONCLUSIONS

We have discussed whether the coupled-channels analysis of the fusion reaction of the $^{74}$Ge + $^{74}$Ge and $^{72}$Ge + $^{72}$Ge systems can probe the characteristic properties of the structure of $^{72,74}$Ge nuclei suggested by the experiments of Coulomb excitation. The present calculations clearly show that the fusion barrier distribution analysis can be used to probe the structure of these nuclei.

We have shown that the fusion barrier distribution for the $^{74}$Ge + $^{74}$Ge reactions calculated by assuming the coupling matrix given by the Coulomb excitation experiments noticeably differs from that obtained with the rotational model, but agrees in a much better way with the results of the vibrational coupling model. In that sense, $^{74}$Ge is more likely to be a spherical nucleus than a deformed nucleus. This finding agrees with the result of previous analysis of the fusion reactions for $^{16}$O,$^{27}$Al + $^{74}$Ge [16] and $^{74}$Ge + $^{74}$Ge [17,18] systems. It will be interesting if high precision experiments can be performed to measure the fusion cross section and if the fusion barrier distribution is extracted in order to compare with the results predicted by the data of Coulomb excitation. Precise new data are highly desirable, since the previous data [15,29] have a large uncertainties which make it difficult to extract the fusion barrier distribution.

From the analyses of the $^{72}$Ge + $^{72}$Ge fusion reactions, we have shown that the fusion excitation function and the fusion barrier distribution obtained by assuming the coupling matrix suggested by the experiments of Coulomb excitation significantly differ from those obtained in either pure rotational or vibrational models. The experimental coupling matrix, i.e., Eq. (11), is based on the point of view that the $^{72}$Ge has a shape admixture in its ground state, in contrast to the analyses of the $^{16}$O,$^{27}$Al + $^{72}$Ge reactions [16], which favor a prolately deformed shape for $^{72}$Ge and the associated rotational coupling scheme for the coupled-channels calculations. In this connection, we wish to mention that the analysis of $^{16}$O,$^{27}$Al + $^{72}$Ge reactions in Ref. [16] suggested a significantly smaller radius for the $^{72}$Ge nucleus than that predicted from a smooth $A^{1/3}$ interpolation among different Ge isotopes, which we assumed in this paper. Also the $\chi^2$ value is much larger for this isotope than that for the other isotopes, especially for the $^{16}$O + $^{72}$Ge fusion reactions. Furthermore, the $\chi^2$ values for the rotational and the vibrational models do not differ so much. These might be the indications of the shape admixed property of this nucleus. Likewise for the $^{74}$Ge + $^{74}$Ge reactions, it will be very interesting to experimentally determine the fusion barrier distribution for the $^{72}$Ge + $^{72}$Ge as well as other $^{72}$Ge based reactions. It will certainly shed light on the shape properties of the $^{72}$Ge nucleus in addition to the experiments of the Coulomb excitation. Also, it is highly desirable to have experimental data for the missing elements in the matrix in Eq. (11), and also for the coupling of $2_1^+$ state to the $2_2^+$ and $4_1^+$ states and the quadrupole moment of the $4_1^+$ state. They will enable us to perform the coupled-channels calculations with less ambiguity. To the contrary, if the data of the fusion barrier distribution are available, they will provide us with the information on these missing coupling matrices.

## ACKNOWLEDGMENTS

The authors are thankful to Dr. M. Oshima for useful information on the data of Coulomb excitation. This work is one of the Channel System Programs of the Egyptian government. N.T. and Z.M.M.M. acknowledge the program. This work was supported by the Japanese Ministry of Education, Culture, Sports, Science and Technology by Grant-in-Aid for Scientific Research under the Program No. 19740115. M.Z.F. acknowledges support from Universitas Haluoleo.

[1] A. B. Balantekin and N. Takigawa, Rev. Mod. Phys. **70**, 77 (1998).
[2] M. Dasgupta, D. J. Hinde, and A. M. Stefanini, Annu. Rev. Nucl. Part. Sci. **48**, 401 (1998).
[3] L. F. Canto, P. R. S. Gomes, R. Donangelo, and M. S. Hussein, Phys. Rep. **424**, 1 (2006).
[4] N. Keeley, R. Raabe, N. Alamanos, and J. L. Sida, Prog. Part. Nucl. Phys. **59**, 579 (2007).
[5] J. R. Leigh, M. Dasgupta, D. J. Hinde, J. C. Mein, C. R. Morton, R. C. Lemmon, J. P. Lestone, J. O. Newton, H. Timmers, J. X. Wei, and N. Rowley, Phys. Rev. C **52**, 3151 (1995).
[6] N. Rowley, G. R. Sacthler, and P. H. Stelson, Phys. Lett. B **254**, 25 (1991).
[7] *Table of Isotopes*, 8th ed., edited by R. B. Firestone and V. S. Shirley (John Wiley and Sons, New York, 1996).
[8] J. Dobaczewski, W. Nazarewicz, J. Skalski, and T. Werner, Phys. Rev. Lett. **60**, 2254 (1988).
[9] M. M. Sharma, M. A. Nagarajan, and P. Ring, Phys. Lett. B **312**, 377 (1993).
[10] R. Lecomte, M. Irshad, S. Landsberger, P. Paradis, and S. Monaro, Phys. Rev. C **22**, 1530 (1980).
[11] R. Lecomte, M. Irshad, S. Landsberger, G. Kajrys, P. Paradis, and S. Monaro, Phys. Rev. C **22**, 2420 (1980).
[12] Y. Toh, T. Czosnyka, M. Oshima, T. Hayakawa, H. Kusakari, M. Sugawara, Y. Tuscany, J. Katakura, N. Shinohara, and M. Matsuda, Eur. Phys. J. A **9**, 353 (2000).
[13] M. Sugawara, Y. Toh, T. Czosnyka, M. Oshima, T. Hayakawa, H. Kusakari, Y. Hatsukawa, J. Katakura, N. Shinohara, M. Matsuda, T. Morikawa, A. Seki, and F. Sakata, Eur. Phys. J. A **16**, 409 (2003).
[14] E. F. Aguilera, J. J. Kolata, and R. J. Tighe, Phys. Rev. C **52**, 3103 (1995).
[15] E. F. Aguilera, J. J. Vega, J. J. Kolata, A. Morsad, R. G. Tighe, and X. J. Kong, Phys. Rev. C **41**, 910 (1990).
[16] H. Esbensen, Phys. Rev. C **68**, 034604 (2003).
[17] H. Esbensen, Phys. Rev. C **72**, 054607 (2005).
[18] H. Esbensen and S. Misicu, AIP Conf. Proc. **853**, 13 (2006).
[19] C. E. Aguiar, V. C. Barbosa, L. F. Canto, and R. Donangelo, Phys. Lett. B **201**, 22 (1988).
[20] A. Iwamoto and N. Takigawa, Phys. Lett. B **219**, 176 (1989).
[21] N. Takigawa, Zakarya Mohamed Mohamed Mahmoed, F. Muhammad Zamrun, Nyeink Wink Lwin, T. Takehi, and K. Hagino, Nucl. Phys. A **787**, 190c (2007).
[22] N. Takigawa and K. Ikeda, in *Proceedings of the Symposium on Many Facets of Heavy Ion Fusion Reactions*, edited by W. Henning *et al.* (Argonne National Laboratory Report No. ANL-PHY-87-1, 1986), p. 613.

[23] H. Esbensen, S. Landowne, and C. Price, Phys. Rev. C **36**, 1216 (1987); **36**, 2359 (1987).
[24] K. Hagino, N. Rowley, and A. T. Kruppa, Comput. Phys. Commun. **123**, 143 (1999).
[25] O. Akyüz and A. Winther, in Proceedings of the Enrico Fermi School of Physics, 1979, Course on *Nuclear Structure and Heavy Ions Reactions*, edited by R. A. Broglia, C. H. Dasso, and R. Ricci (North Holland, Amsterdam, 1981).
[26] R. A. Broglia and A. Winther, *Frontier in Physics Lecture Notes Series; Heavy Ion Reactions* (Addison-Wesley, Redwood City, CA, 1991), Vol. 84.
[27] P. R. Christensen and A. Winther, Phys. Lett. B **65**, 19 (1976).
[28] G. R. Sacthler and W. G. Love, Phys. Rep. **55**, 183 (1979).
[29] M. Beckerman, M. K. Salomaa, J. Wiggins, and R. Rohe, Phys. Rev. C **28**, 1963 (1983).
[30] A. M. Stefanini, L. Corradi, A. M. Vinodkumar, Yang Feng, F. Scarlassara, G. Montagnoli, S. Beghini, and M. Bisogno, Phys. Rev. C **62**, 014601 (2000).
[31] J. O. Newton, C. R. Morton, M. Dasgupta, J. R. Leigh, J. C. Mein, D. J. Hinde, H. Timmers, and K. Hagino, Phys. Rev. C **64**, 064608 (2001).
[32] H. Timmers, D. Ackermann, S. Beghini, L. Corradi, J. H. He, G. Montagnoli, E. Scarlassara, A. M. Stefanini, and N. Rowley, Nucl. Phys. A **633**, 421 (1998).
[33] T. Kibedi and R. H. Spear, At. Data Nucl. Data Tables **80**, 35 (2002).